

# EFFECTS OF FRUSTRATED SURFACE IN HEISENBERG THIN FILMS

V. Thanh Ngo<sup>a,b</sup> and H. T. Diep<sup>a\*</sup>

<sup>a</sup> *Laboratoire de Physique Théorique et Modélisation, CNRS-Université de Cergy-Pontoise, UMR 8089 5, mail Gay-Lussac, Neuville sur Oise, 95031 Cergy-Pontoise Cedex, France*

<sup>b</sup> *Institute of Physics, P.O. Box 429 Bo Ho, Hanoi 10000, Vietnam*

We study by extensive Monte Carlo (MC) simulations and analytical Green function (GF) method effects of frustrated surfaces on the properties of thin films made of stacked triangular layers of atoms bearing Heisenberg spins. The film surfaces are frustrated due to antiferromagnetic in-plane interactions  $J_s$ , while interior layers are ferromagnetic. The ground-state spin configuration is found non collinear below a critical value of  $J_s$ . In general, there are two phase transitions related to surface and interior disorderings. The MC and GF results agree qualitatively. We have also included the cohesive interactions between neighboring atoms. The magnetic and cohesive interactions are supposed to be the distance-dependent Lennard-Jones (LJ) potential. Results on various properties are shown and discussed.

PACS numbers:

## I. INTRODUCTION

This paper deals with the effect of the frustration in magnetic thin films. The frustration is known to cause spectacular effects in various bulk spin systems. Its effects have been extensively studied during the last decade theoretically, experimentally and numerically. Frustrated model systems serve not only as testing ground for theories and approximations, but also to compare with experiments.<sup>1</sup>

On the other hand, surface physics and systems of nanoscales have been also enormously studied during the last twenty years. This is due in particular to applications in magnetic recording, let alone fundamental theoretical interests. Much is understood theoretically and experimentally in thin films where surfaces are 'clean' i.e. no impurities, no steps etc.<sup>2,3,4,5,6</sup> Less is known at least theoretically on complicated thin films with special surface conditions such as defects<sup>7,8</sup>, arrays of dots and magnetization reversal phenomenon.<sup>9,10,11,12,13,15,16</sup>

In this paper we study the frustration effect on properties of thin films made of stacked triangular lattices. In-plane interaction of the surfaces is antiferromagnetic and that of interior layers is ferromagnetic. The film surfaces are frustrated. We also take into account the motions of atoms around their equilibrium positions. Magnetic and cohesive interactions are thus included.

The paper is organized as follows. Section II is devoted to the description of our model. In section III, we consider the case of magnetic interaction only on rigid lattice. We are interested in the effect of magnetic frustration alone on magnetic properties of thin films. The ground-state spin configuration is determined as a function of surface interaction. A phase diagram is established showing interesting surface behaviors. Results from Monte Carlo simulations and from the Green func-

tion method are compared. Section IV is devoted to the case where both magnetic and cohesive interactions are taken into account. This is an off-lattice model because atoms are allowed to move. Concluding remarks are given in Section V.

## II. LATTICE MODEL

It is known that many established theories failed to deal with frustrated spin systems.<sup>1</sup> Among known striking effects due to frustration, let us mention the high ground-state (GS) degeneracy associated often with new symmetries which give rise sometimes to new kinds of phase transition. One of the systems which are most studied is the antiferromagnetic triangular lattice. Due to its geometry, the spins are frustrated under nearest-neighbor (NN) antiferromagnetic interaction. In the case of Heisenberg model, the frustration results in a 120° GS structure: the NN spins form a 120° angle alternately in the clockwise and counter-clockwise senses which are called left and right chiralities.

In this paper we consider a thin film made up by stacking  $N_z$  planes of triangular lattice of  $N \times N$  lattice sites.

The Hamiltonian is given by

$$\mathcal{H} = - \sum_{\langle i,j \rangle} J_{i,j} \mathbf{S}_i \cdot \mathbf{S}_j \quad (1)$$

where  $\mathbf{S}_i$  is the Heisenberg spin at the lattice site  $i$ ,  $\sum_{\langle i,j \rangle}$  indicates the sum over the NN spin pairs  $\mathbf{S}_i$  and  $\mathbf{S}_j$ .

Interaction between two NN surface spins is equal to  $J_s$ . Interaction between layers and interaction between NN in interior layers are supposed to be ferromagnetic and all equal to  $J = 1$  for simplicity. The two surfaces of the film are frustrated if  $J_s$  is antiferromagnetic ( $J_s < 0$ ).

\*Corresponding author, E-mail: diep@ptm.u-cergy.fr

### A. Ground state

For  $J_s > 0$  (ferromagnetic interaction), the magnetic ground state (GS) is ferromagnetic. However, when  $J_s$  is negative the surface spins are frustrated. Therefore, there is a competition between the non collinear surface ordering and the ferromagnetic ordering due to the ferromagnetic interaction from the spins of the beneath layer.

We first determine the GS configuration by using the steepest descent method : starting from a random spin configuration, we calculate the magnetic local field at each site and align the spin of the site in its local field. In doing so for all spins and repeat until the convergence is reached, we obtain in general the GS configuration, without metastable states in the present model. The result shows that when  $J_s$  is smaller than a critical value  $J_s^c$  the magnetic GS is obtained from the planar  $120^\circ$  spin structure, supposed to be in the  $XY$  plane, by pulling them out of the spin  $XY$  plane by an angle  $\beta$ . The three spins on a triangle on the surface form thus an 'umbrella' with an angle  $\alpha$  between them and an angle  $\beta$  between a surface spin and its beneath neighbor (see Fig. 1). This non planar structure is due to the interaction of the spins on the beneath layer, just like an external applied field in the  $z$  direction. Of course, when  $J_s$  is larger than  $J_s^c$  one has the collinear ferromagnetic GS as expected: the frustration is not strong enough to resist the ferromagnetic interaction from the beneath layer.

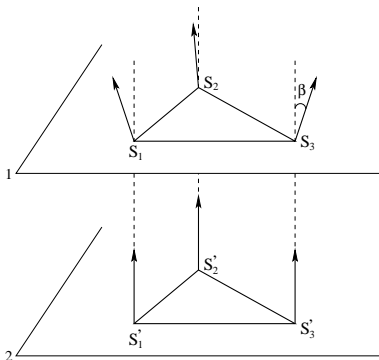


FIG. 1: Non collinear surface spin configuration. Angles between spins on layer 1 are all equal (noted  $\alpha$ ), while angles between vertical spins are  $\beta$ .

We show in Fig. 2  $\cos(\alpha)$  and  $\cos(\beta)$  as functions of  $J_s$ . The critical value  $J_s^c$  is found between -0.10 and -0.11. This value can be calculated analytically by assuming the 'umbrella structure'. For GS analysis, it suffices to consider just a cell shown in Fig.1. This is justified by the numerical determination discussed above. Furthermore, we consider as a single solution all configurations obtained from each other by any global spin rotation.

Let us consider the Hamiltonian (1). The spins are numbered as in Fig. 1:  $S_1$ ,  $S_2$  and  $S_3$  are the spins in the surface layer (first layer),  $S'_1$ ,  $S'_2$  and  $S'_3$  are the spins in the internal layer (second layer). For simplicity,

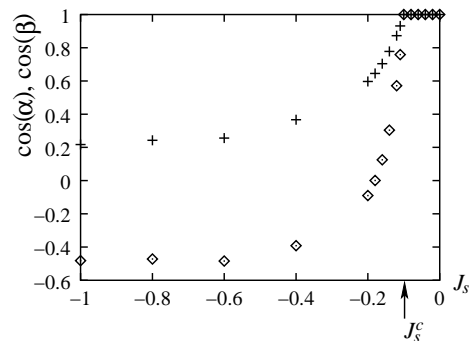


FIG. 2:  $\cos(\alpha)$  (diamonds) and  $\cos(\beta)$  (crosses) as functions of  $J_s$ . Critical value of  $J_s^c$  is shown by the arrow.

the interaction inside the surface layer is set equal  $J_s$  ( $-1 \leq J_s \leq 1$ ) and all others are set equal to  $J$ . The Hamiltonian for the cell is written as

$$H_p = -6 [J_s (\mathbf{S}_1 \cdot \mathbf{S}_2 + \mathbf{S}_2 \cdot \mathbf{S}_3 + \mathbf{S}_3 \cdot \mathbf{S}_1) + J (\mathbf{S}'_1 \cdot \mathbf{S}'_2 + \mathbf{S}'_2 \cdot \mathbf{S}'_3 + \mathbf{S}'_3 \cdot \mathbf{S}'_1)] - J (\mathbf{S}_1 \cdot \mathbf{S}'_1 + \mathbf{S}_2 \cdot \mathbf{S}'_2 + \mathbf{S}_3 \cdot \mathbf{S}'_3), \quad (2)$$

Let us decompose each spin into two components: an  $xy$  component, which is a vector, and a  $z$  component  $\mathbf{S}_i = (\mathbf{S}_i^{\parallel}, S_i^z)$ . Only surface spins have  $xy$  vector components. The angle between these  $xy$  components of NN surface spins is  $\gamma_{i,j}$  which is chosen by ( $\gamma_{i,j}$  is in fact the projection of  $\alpha$  defined above on the  $xy$  plane)

$$\gamma_{1,2} = 0, \quad \gamma_{2,3} = \frac{2\pi}{3}, \quad \gamma_{3,1} = \frac{4\pi}{3}. \quad (3)$$

The angles  $\beta_i$  and  $\beta'_i$  of the spin  $\mathbf{S}_i$  and  $\mathbf{S}'_i$  with the  $z$  axis are by symmetry

$$\begin{cases} \beta_1 = \beta_2 = \beta_3 = \beta, \\ \beta'_1 = \beta'_2 = \beta'_3 = 0, \end{cases}$$

The total energy of the cell (2), with  $S_i = S'_i = \frac{1}{2}$ , can be rewritten as

$$H_p = -\frac{9J}{2} - \frac{3J}{2} \cos \beta - \frac{9J_s}{2} \cos^2 \beta + \frac{9J_s}{4} \sin^2 \beta. \quad (4)$$

By a variational method, the minimum of the cell energy corresponds to

$$\frac{\partial H_p}{\partial \beta} = \frac{27J_s}{2} \cos \beta \sin \beta + \frac{3J}{2} \sin \beta = 0 \quad (5)$$

We have

$$\cos \beta = -\frac{J}{9J_s}. \quad (6)$$

We see that the solution (6) exists for  $J_s \leq J_s^c$  where the critical value  $J_s^c = -\frac{J}{9} \approx -0.11J$  is in excellent agreement with the numerical result.

## B. Green function method

For a given value of  $J_s$ , we shall use the Green function method to calculate the layer magnetizations as functions of temperature. The details of the method in the case of non collinear spin configuration have been given in Ref.<sup>18</sup>. We briefly recall it here and show the application to the present model.

We can rewrite the Hamiltonian in the local framework as

$$\begin{aligned} \mathcal{H} = & - \sum_{\langle i,j \rangle} J_{i,j} \left\{ \frac{1}{4} (\cos \theta_{ij} - 1) (S_i^+ S_j^+ + S_i^- S_j^-) \right. \\ & + \frac{1}{4} (\cos \theta_{ij} + 1) (S_i^+ S_j^- + S_i^- S_j^+) \\ & + \frac{1}{2} \sin \theta_{ij} (S_i^+ + S_i^-) S_j^z - \frac{1}{2} \sin \theta_{ij} S_i^z (S_j^+ + S_j^-) \\ & \left. + \cos \theta_{ij} S_i^z S_j^z \right\}, \end{aligned} \quad (7)$$

where  $\cos(\theta_{ij})$  is the angle between two NN spins.

Following Tahir-Kheli and ter Haar,<sup>14</sup> we define two double-time Green functions by

$$G_{ij}(t, t') = \ll S_i^+(t); S_j^-(t') \gg, \quad (8)$$

$$F_{ij}(t, t') = \ll S_i^-(t); S_j^+(t') \gg. \quad (9)$$

The equation of motion for  $G_{ij}(t, t')$  and  $F_{ij}(t, t')$  reads

$$\begin{aligned} i \frac{d}{dt} G_{i,j}(t, t') &= \langle [S_i^+(t), S_j^-(t')] \rangle \delta(t - t') \\ &\quad - \langle \langle [\mathcal{H}, S_i^+(t)]; S_j^-(t') \rangle \rangle, \end{aligned} \quad (10)$$

$$\begin{aligned} i \frac{d}{dt} F_{i,j}(t, t') &= \langle [S_i^-(t), S_j^+(t')] \rangle \delta(t - t') \\ &\quad - \langle \langle [\mathcal{H}, S_i^-(t)]; S_j^+(t') \rangle \rangle, \end{aligned} \quad (11)$$

We neglect higher order correlations by using the Tyablikov decoupling scheme<sup>17</sup> which is known to be valid for exchange terms.<sup>19</sup> Then, we introduce the Fourier transforms

$$G_{i,j}(t, t') = \frac{1}{\Delta} \int \int d\mathbf{k}_{xy} \frac{1}{2\pi} \int_{-\infty}^{+\infty} d\omega e^{-i\omega(t-t')} g_{n,n'}(\omega, \mathbf{k}_{xy}) e^{i\mathbf{k}_{xy} \cdot (\mathbf{R}_i - \mathbf{R}_j)}, \quad (12)$$

$$F_{i,j}(t, t') = \frac{1}{\Delta} \int \int d\mathbf{k}_{xy} \frac{1}{2\pi} \int_{-\infty}^{+\infty} d\omega e^{-i\omega(t-t')} f_{n,n'}(\omega, \mathbf{k}_{xy}) e^{i\mathbf{k}_{xy} \cdot (\mathbf{R}_i - \mathbf{R}_j)}, \quad (13)$$

where  $\omega$  is the spin-wave frequency,  $\mathbf{k}_{xy}$  denotes the wave-vector parallel to  $xy$  planes,  $\mathbf{R}_i$  is the position of the spin at the site  $i$ ,  $n$  and  $n'$  are respectively the index of the layers where the sites  $i$  and  $j$  belong to. The integral over  $\mathbf{k}_{xy}$  is performed in the first Brillouin zone whose surface is  $\Delta$  in the  $xy$  reciprocal plane.

The Fourier transforms of the retarded Green functions satisfy a set of equations rewritten under a matrix form

$$\mathbf{M}(\omega) \mathbf{g} = \mathbf{u}, \quad (14)$$

in here,  $\mathbf{M}(\omega)$  is a square matrix ( $2N_T \times 2N_T$ ),  $\mathbf{g}$  and  $\mathbf{u}$  are the column matrices which are defined as follows

$$\mathbf{g} = \begin{pmatrix} g_{1,n'} \\ f_{1,n'} \\ \vdots \\ g_{N_T,n'} \\ f_{N_T,n'} \end{pmatrix}, \quad \mathbf{u} = \begin{pmatrix} 2 \langle S_1^z \rangle \delta_{1,n'} \\ 0 \\ \vdots \\ 2 \langle S_{N_T}^z \rangle \delta_{N_T,n'} \\ 0 \end{pmatrix}, \quad (15)$$

and

$$\mathbf{M}(\omega) = \begin{pmatrix} A_1^+ & B_1 & D_1^+ & D_1^- & \cdots \\ -B_1 & A_1^- & -D_1^- & -D_1^+ & \vdots \\ \vdots & \cdots & \cdots & \cdots & \vdots \\ \vdots & C_{N_T}^+ & C_{N_T}^- & A_{N_T}^+ & B_{N_T} \\ \cdots & -C_{N_T}^- & -C_{N_T}^+ & -B_{N_T} & A_{N_T}^- \end{pmatrix}, \quad (16)$$

where

$$\begin{aligned} A_n^\pm &= \omega \pm \left[ \frac{1}{2} J_n \langle S_n^z \rangle (Z\gamma) (\cos \theta_n - 1) \right. \\ &\quad \left. - J_n \langle S_n^z \rangle Z \cos \theta_n - J_{n,n+1} \langle S_{n+1}^z \rangle \cos \theta_{n,n+1} \right. \\ &\quad \left. - J_{n,n-1} \langle S_{n-1}^z \rangle \cos \theta_{n,n-1} \right], \end{aligned} \quad (17)$$

$$B_n = \frac{1}{2} J_n \langle S_n^z \rangle (\cos \theta_n - 1) (Z\gamma), \quad (18)$$

$$C_n^\pm = \frac{1}{2} J_{n,n-1} \langle S_n^z \rangle (\cos \theta_{n,n-1} \pm 1), \quad (19)$$

$$D_n^\pm = \frac{1}{2} J_{n,n+1} \langle S_n^z \rangle (\cos \theta_{n,n+1} \pm 1), \quad (20)$$

in which,  $Z = 6$  is the number of in-plane NN,  $\theta_{n,n\pm 1}$  the angle between two spins belonging to the layers  $n$  and  $n \pm 1$ ,  $\theta_n$  the angle between two in-plane NN in the layer  $n$ , and

$$\gamma = \left[ 2 \cos(k_x a) + 4 \cos(k_y a/2) \cos(k_y a \sqrt{3}/2) \right] / Z.$$

Solving  $\det|\mathbf{M}| = 0$ , we obtain the spin-wave spectrum  $\omega$  of the present system. The solution for the Green function  $g_{n,n}$  is given by

$$g_{n,n} = \frac{|\mathbf{M}|_n}{|\mathbf{M}|}, \quad (21)$$

with  $|\mathbf{M}|_n$  is the determinant made by replacing the  $n$ -th column of  $|\mathbf{M}|$  by  $\mathbf{u}$  in (15). Writing now

$$|\mathbf{M}| = \prod_i (\omega - \omega_i(\mathbf{k}_{xy})), \quad (22)$$

one sees that  $\omega_i(\mathbf{k}_{xy})$ ,  $i = 1, \dots, N_T$ , are poles of the Green function  $g_{n,n}$ .  $\omega_i(\mathbf{k}_{xy})$  can be obtained by solving  $|\mathbf{M}| = 0$ . In this case,  $g_{n,n}$  can be expressed as

$$g_{n,n} = \sum_i \frac{f_n(\omega_i(\mathbf{k}_{xy}))}{(\omega - \omega_i(\mathbf{k}_{xy}))}, \quad (23)$$

where  $f_n(\omega_i(\mathbf{k}_{xy}))$  is

$$f_n(\omega_i(\mathbf{k}_{xy})) = \frac{|\mathbf{M}|_n(\omega_i(\mathbf{k}_{xy}))}{\prod_{j \neq i} (\omega_j(\mathbf{k}_{xy}) - \omega_i(\mathbf{k}_{xy}))}. \quad (24)$$

Next, using the spectral theorem which relates the correlation function  $\langle S_i^- S_j^+ \rangle$  to the Green functions,<sup>20</sup> one has

$$\begin{aligned} \langle S_i^- S_j^+ \rangle &= \lim_{\epsilon \rightarrow 0} \frac{1}{\Delta} \int \int d\mathbf{k}_{xy} \int_{-\infty}^{+\infty} \frac{i}{2\pi} (g_{n,n'}(\omega + i\epsilon) \\ &- g_{n,n'}(\omega - i\epsilon)) \cdot \frac{d\omega}{e^{\beta\omega} - 1} e^{i\mathbf{k}_{xy} \cdot (\mathbf{R}_i - \mathbf{R}_j)}, \end{aligned} \quad (25)$$

where  $\epsilon$  is an infinitesimal positive constant and  $\beta = 1/k_B T$ ,  $k_B$  being the Boltzmann constant.

Using the Green function presented above, we can calculate self-consistently various physical quantities as functions of temperature  $T$ . The first important quantity is the temperature dependence of the angle between each spin pair. This can be calculated in a self-consistent manner at any temperature by minimizing the free energy at each temperature to get the correct value of the angle as it has been done for a frustrated bulk spin systems.<sup>21</sup> In this paper, we limit ourselves to the self-consistent calculation of the layer magnetizations which allows us to establish the phase diagram as seen in the following.

For numerical calculation, we used a size of  $80^3$  points in the first Brillouin zone starting the self-consistent calculation from  $T = 0$  with a small step for temperature  $5 \times 10^{-3}$  or  $10^{-1}$  (in units of  $J/k_B$ ). The convergence precision has been fixed at the fourth figure of the values obtained for the layer magnetizations.

### C. Phase transition and phase diagram of the quantum case

We first show an example where  $J_s = -0.5$  in Fig. 3. As seen, the surface-layer magnetization is much smaller than the second-layer one. In addition there is a strong spin contraction at  $T = 0$  for the surface layer. This is due to the antiferromagnetic nature of the in-plane surface interaction  $J_s$ . One sees that the surface becomes disordered at a temperature  $T_1 \simeq 0.22$  while the second layer remains ordered up to  $T_2 \simeq 1.24$ . Therefore, the system is partially disordered for temperatures between  $T_1$  and  $T_2$ . This result is very interesting because it confirms again the existence of the partial disorder in quantum spin systems observed earlier in bulk frustrated quantum spin systems.<sup>18,21</sup>

We show in Fig. 4 the phase diagram in the space  $(J_s, T)$ . Phases I and II denote respectively the canted spin state and the ferromagnetic state, phase III indicates the partially disordered state where surface spins are disordered, and phase IV is the paramagnetic phase.

Note that the surface is disordered down to  $T = 0$  at  $J_s^c$ .

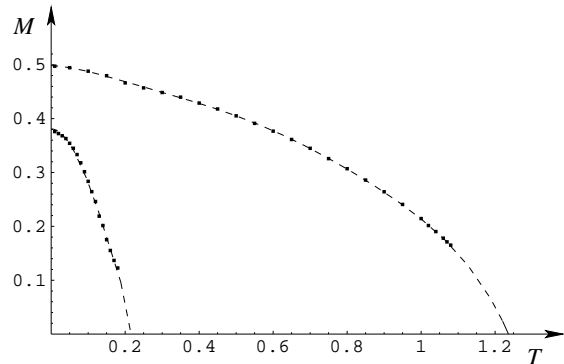


FIG. 3: First two layer-magnetizations obtained by the Green function technique vs.  $T$  for  $J_s = -0.5$ . The surface-layer magnetization (lower curve) is much smaller than the second-layer one. See text for comments.

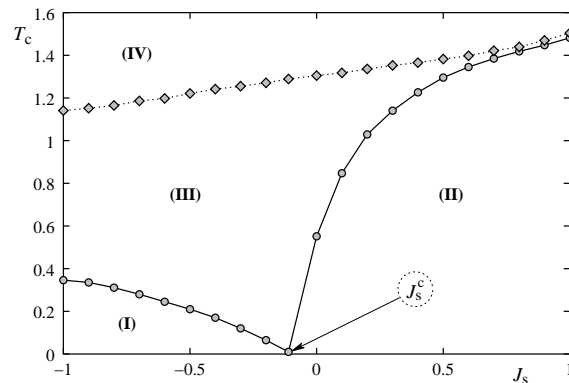


FIG. 4: Phase diagram in the space  $(J_s, T)$  for the quantum Heisenberg model with  $N_z = 4$ . See text for the description of phases I to IV.

### D. Monte Carlo results

In this paragraph, we show the results obtained by MC simulations with the Hamiltonian 1 but the spins are the classical Heisenberg model of magnitude  $S = 1$ .

The film sizes are  $N \times N \times N_z$  where  $N_z$  is the number of layers (film thickness). We use here  $N = 12$  to  $30$  and  $N_z = 4$  as in the quantum case presented above. Periodic boundary conditions are used in the  $XY$  planes. The equilibrating time is about  $10^6$  MC steps per spin and the averaging time is  $10^6 - 2 \times 10^6$  MC steps per spin.  $J = 1$  is taken as unit of energy in the following.

Let us show in Fig. 5 the layer magnetization of the first two layers as a function of  $T$ , in the case  $J_s = 0.5$  with  $N_z = 4$  (the third and fourth layers are symmetric). The surface layer becomes disordered at a temperature lower than that for the second layer.

In Fig. 6 we show a frustrated case where  $J_s = -0.5$ . The surface layer in this case becomes disordered at a temperature much lower than that for the second layer. Note that the surface magnetization is not saturated to

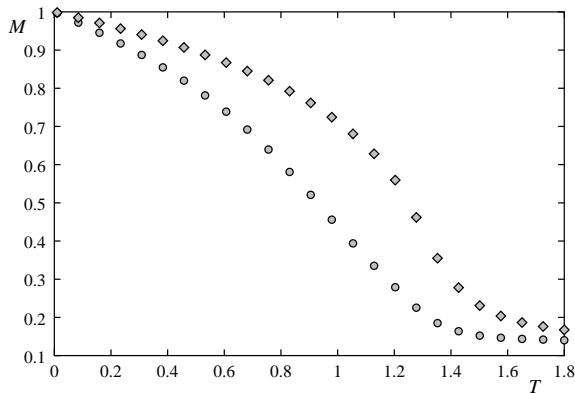


FIG. 5: Magnetizations of layer 1 (cycles) and layer 2 (diamonds) versus temperature  $T$  in unit of  $J/k_B$  for  $J_s = 0.5$ .

1 at  $T = 0$ . This is because the surface spins make an angle with the  $z$  axis so their  $z$  component is less than 1 in the GS.

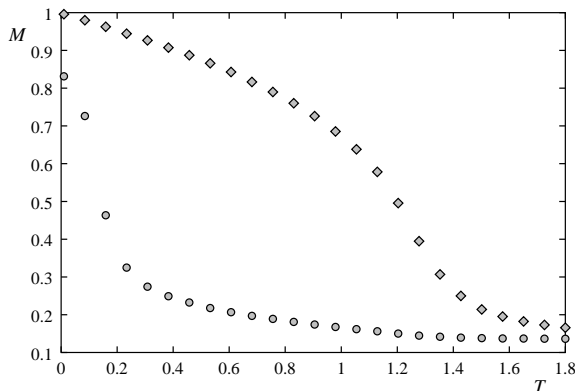


FIG. 6: Magnetizations of layer 1 (cycles) and layer 2 (diamonds) versus temperature  $T$  in unit of  $J/k_B$  for  $J_s = -0.5$ .

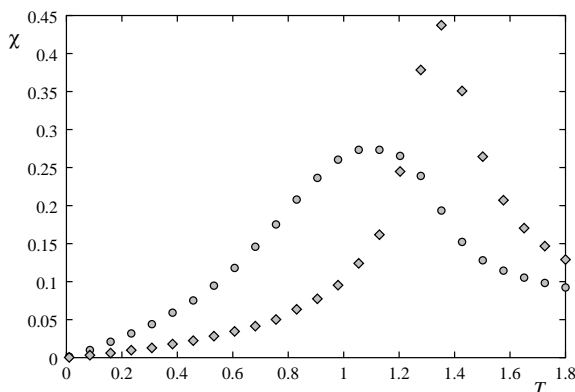


FIG. 7: Susceptibility of layer 1 (cycles) and layer 2 (diamonds) versus temperature  $T$  in unit of  $J/k_B$  for  $J_s = 0.5$ .

To establish the phase diagram, the transition temper-

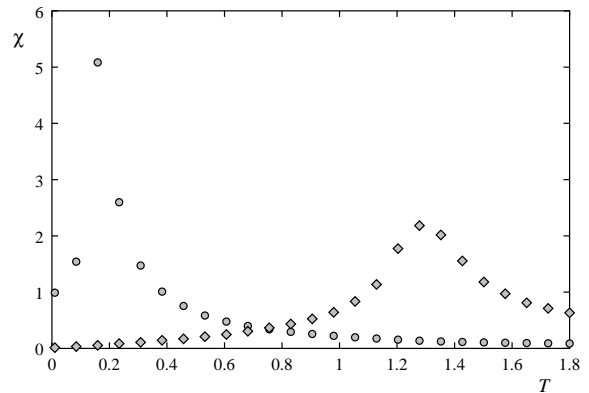


FIG. 8: Susceptibility of layer 1 (cycles) and layer 2 (diamonds) versus temperature  $T$  in unit of  $J/k_B$  for  $J_s = -0.5$ . Note that for clarity, the susceptibility of the layer 2 has been multiplied by a factor 5.

atures are taken at the change of curvature of the layer magnetizations, i.e. at the maxima of layer susceptibilities shown before. Figure 9 shows the phase diagram obtained in the space  $(J_s, T)$ . Interesting enough, this phase diagram resembles remarkably to that obtained for the quantum counterpart model shown in Fig. 4.

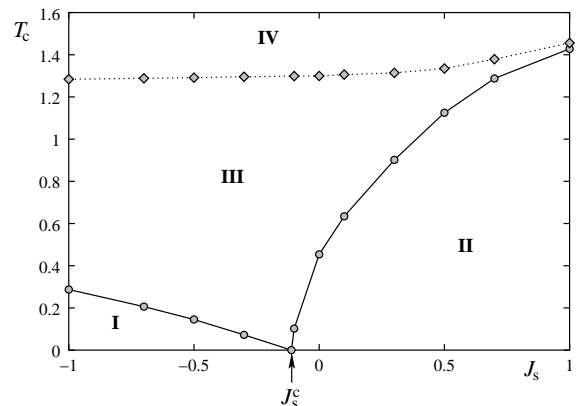


FIG. 9: Phase diagram in the space  $(J_s, T)$  for the classical Heisenberg model with  $N_z = 4$ . Phases I to IV have the same meanings as those in Fig. 4.

### III. OFF-LATTICE MODEL: MAGNETO-ELASTIC INTERACTION

In this section, we show results obtained by MC simulations in the case where both magnetic and elastic interactions are taken into account.

The atoms occupying the lattice sites bear Heisenberg classical spins. They can move around their equilibrium positions. The Hamiltonian is given by

$$\mathcal{H} = \sum_{(ij)} U(r_{ij}) + \sum_{(ij)} J(r_{ij}) \mathbf{S}_i \cdot \mathbf{S}_j \quad (26)$$

where the elastic interaction between atoms at  $\mathbf{r}_i$  and  $\mathbf{r}_j$  is described by the potential  $U(r_{ij})$  and the magnetic interaction by the second term. The spin  $\mathbf{S}_i$  is defined as a unit vector at the  $i$ -th site. The interaction between spins at the sites  $i$  and  $j$  is defined as  $J(r_{ij})$ . For simplicity, the distance dependence of both the elastic and magnetic interactions is supposed to be given by the Lennard-Jones (LJ) potential

$$U(r_{ij}) = U_c \left[ (r_0/r_{ij})^{12} - 2(r_0/r_{ij})^6 \right] \quad (27)$$

$$J(r_{ij}) = U_m \left[ (r_0/r_{ij})^{12} - 2(r_0/r_{ij})^6 \right] \quad (28)$$

where  $r_{ij} = |\mathbf{r}_i - \mathbf{r}_j|$ ,  $r_0$  being the equilibrium distance between two NN atoms which is taken to be 1 in the following. Note that the elastic LJ interaction with positive  $U_c$  is repulsive at short distances while it is attractive for distances larger than  $r_c$  [see Fig. 10]. So the repulsive character will prevent the atoms from collapsing. We show in Fig. 10 the LJ potential  $U(r_{ij})$ .

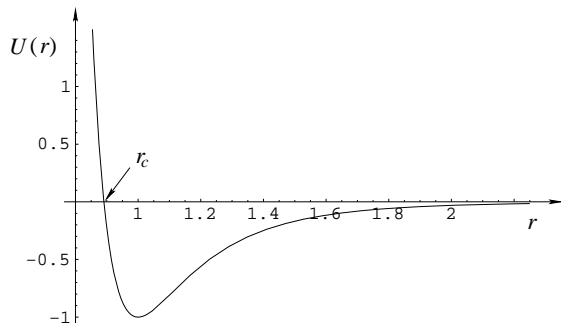


FIG. 10: Lennard-Jones potential chosen in this work with  $U_c = 1$ . For  $r < r_c$  ( $r_c \simeq 0.89$ ),  $U(r)$  is positive (repulsive interaction).

In the Ising case, the magnetic interaction with positive  $U_m$  yields ferromagnetic ordering for  $r > r_c$  and antiferromagnetic ordering for  $r < r_c$ . Therefore the magnetic interaction, unlike the elastic coupling, can allow the formation of short-distance antiferromagnetic spin pairs. The magnetic collapse however can be avoided if the elastic repulsive interaction is larger in magnitude than the negative magnetic energy of those antiferromagnetic spin pairs. If  $U_m$  is not very small with respect to  $U_c$ , there is thus a possibility of formation of antiferromagnetic Ising spin pairs at short distances which have been observed in the bulk systems.<sup>22</sup>

In this section,  $U_c$  is supposed to be much larger than  $U_m$  as usually the case in solid materials. As a consequence, the magnetic phase transition occurs at a temperature much lower than the melting transition. From this observation, we can suppose that for temperatures up to the magnetic transition, atoms are moving inside a

sphere of radius  $D$ . Although this hypothesis is simple, it is known that such a limited motion causes already interesting critical behaviors in bulk spin systems.<sup>22</sup>

We suppose all interactions are limited to NN atoms with their instantaneous positions. The shortest distance between them is thus  $r_0 - 2D$  and the largest one is  $r_0 + 2D$ . To be coherent with the assumption of NN interaction,  $D$  should be taken to be smaller than  $0.183r_0$ . In this work we take  $D = 0.18$  (in unit of  $r_0$ ) except otherwise stated. Furthermore, for magnetic interactions, we suppose that  $U_m$  is positive and is the same everywhere except inside the two surface layers (intra surface-plane interaction) where it is equal to  $U_{ms}$  which is negative. Positive  $U_m$  means that the interaction is ferromagnetic if the spins are no closer than  $r_c \simeq 0.89$ . Negative  $U_{ms}$  imposes an antiferromagnetic interaction for  $r > r_c$ . For the calculation shown hereafter, we take  $U_c = 1.5$  and  $U_m = 1$ .  $U_{ms}$  can be negative or positive.

In MC simulations, the update is made simultaneously for both position and spin orientation. As before, the film sizes are  $N \times N \times N_z$  with  $N = 12$  to 30 and  $N_z = 4$  to 8. Periodic boundary conditions are used in the  $XY$  planes. The equilibrating time is about 50000 MC steps per atom and the averaging time is 100000 MC steps per atom. For our purpose, these run times are found to be sufficient (insufficient if we wish to calculate critical exponents).

The results for the layer magnetization versus  $T$  in the case  $N_z = 4$  do not vary significantly with respect to those obtained in the lattice model shown before for all  $U_{ms}$  from -1 to 1. We emphasize that we did not attempt to determine the criticality of the phase transition. This is interesting but is out of the scope of this work. The magnetic phase diagram in the space  $(U_{ms}, T)$  is therefore very similar with that obtained in the lattice model. These results can be understood by the fact that although atoms are moving around their equilibrium positions, the magnetic energy does not vary much because magnetic interaction potential is more flat around its minimum than the cohesive potential.

We discuss now the effect of  $T$  on the distances between atoms. While the in-plane NN distances increase slowly with increasing  $T$ , the surface-layer one  $d_s$  is slightly larger than that of the interior layer  $d_i$ . We show in Fig.11 these quantities for  $U_{ms} = -0.01$  at  $T = 1$ .

On the other hand, the distance between the surface layer and the second layer  $d_{12}$  is much larger than the one between the second layer and the third layer  $d_{23}$ . Figure 12 at  $T = 1$ .

At this stage, it is interesting to consider the case where surface atoms are allowed to move more freely, i. e. the sphere in which they move has a larger radius  $D$ , for example  $D = 0.25$ . Our results show that the layer magnetizations versus  $T$  still do not vary. However, the distances between surface atoms change considerably. We show these quantities in Figs. 13 and 14 at  $T = 1$ .

The case of  $N_z = 8$  has the same features as those for  $N_z = 4$  shown above, except that the transition temper-

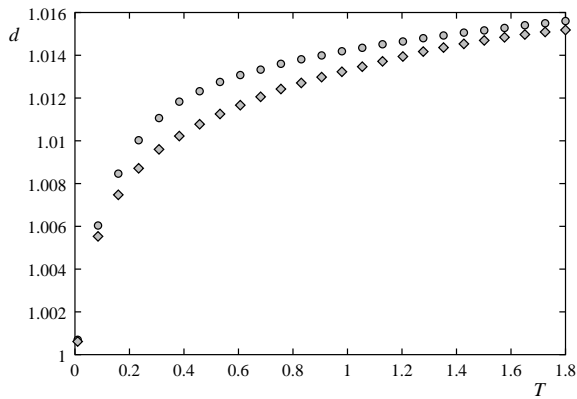


FIG. 11: Distance between two NN atoms in the surface layer (upper curve) and in the second layer (lower curve).  $N_z = 4$ ,  $T = 1$ ,  $U_{ms} = -0.01$ .

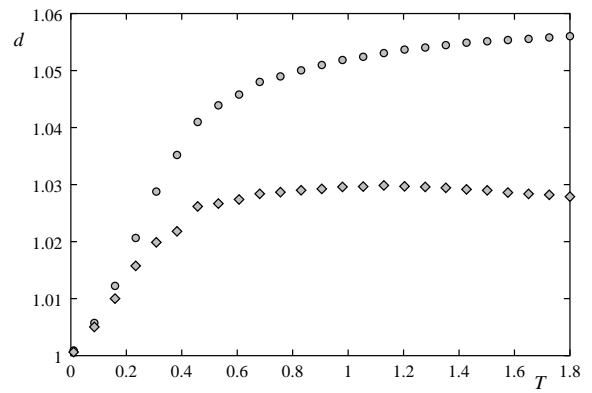


FIG. 14: Distance between two NN atoms in two adjacent layers:  $d_{12}$  (upper curve) and  $d_{23}$  (lower curve) with  $D = 0.25$ ,  $N_z = 4$ ,  $T = 1$ ,  $U_{ms} = -0.01$ .

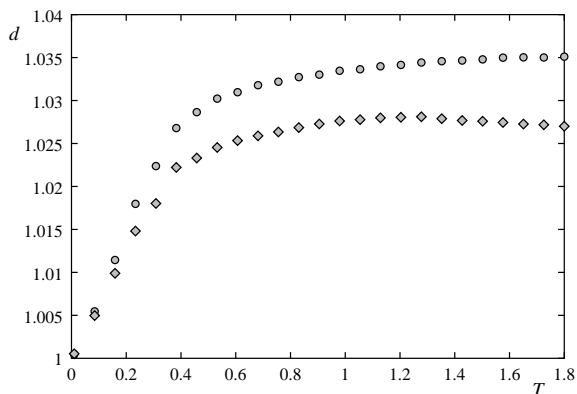


FIG. 12: Distance between two NN atoms in two adjacent layers:  $d_{12}$  (upper curve) and  $d_{23}$  (lower curve).  $N_z = 4$ ,  $T = 1$ ,  $U_{ms} = -0.01$ .

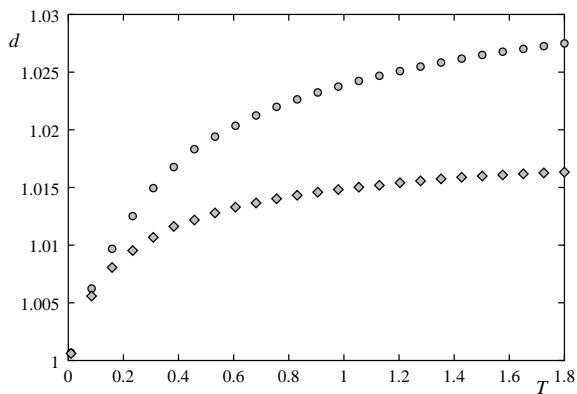


FIG. 13: Distance between two NN atoms in the surface layer (upper curve) and in the second layer (lower curve) with  $D = 0.25$ ,  $N_z = 4$ ,  $T = 1$ ,  $U_{ms} = -0.01$ .

ature is higher as expected.

Let us discuss on the case where  $U_c$  is only slightly larger than  $|U_m|$ . As observed in the bulk case,<sup>22</sup> we find

here that some atoms can get very close to each other because their repulsive positive energy is compensated by the fact that the spins of those atom pairs can be ordered antiferromagnetically giving rise to negative magnetic energy. These contracted antiferromagnetic spin pairs break the surface periodicity causing a surface melting when the constraint on the value of  $D$  is removed (atoms are allowed to move freely). This is seen by the distance histogram taken during the simulations.

#### IV. CONCLUDING REMARKS

We have studied the Heisenberg spin model in thin films of stacked triangular lattices whose surface layers are frustrated, by means of a Green function method and MC simulations. Using a lattice model, we found that surface spin configuration is non collinear when surface antiferromagnetic interaction amplitude is larger than a critical value  $J_s^c$ . The surface layer is disordered in general at a temperature lower than that for interior layers ('soft' surface). A phase diagram is established in the space  $(T, J_s)$ . An excellent agreement between the Green function method and the MC simulation is observed. The phase diagram shows a region where the surface is disordered while the interior spins are ordered. In particular, at the critical value  $J_s^c$ , the surface is disordered down to  $T = 0$ . This can explain the so-called 'magnetically dead surface' observed in some materials.<sup>23,24</sup> We have also considered an off-lattice model where atomic motions are taken into account. One of the most interesting aspects found here is the temperature-dependence of the distance between atoms which is different according to their positions with respect to the surface. The magneto-elastic coupling plays certainly a very important role when we leave the atoms to move freely. The nature of the surface melting may be then affected by the presence of the magnetic interaction. This is a formidable task which is out the the scope of this work.

One of us (NVT) thanks 'World Laboratory' for financial support. This work is supported by a contract

between CNRS (France) and NCST (Vietnam).

- 
- <sup>1</sup> See reviews on theories and experiments given in *Magnetic Systems with Competing Interactions (Frustrated Spin Systems)*, ed. H. T. Diep, World Scientific (1994).
- <sup>2</sup> K. Binder, in *Phase Transitions and Critical Phenomena*, ed. by C. Domb, J.L. Lebowitz (Academic, London, 1983) vol. 8.
- <sup>3</sup> H.W. Diehl, in *Phase Transitions and Critical Phenomena*, ed. by C. Domb, J.L. Lebowitz (Academic, London, 1986) vol. 10, H.W. Diehl, Int. J. Mod. Phys. B **11**, 3503 (1997).
- <sup>4</sup> H. T. Diep, J.C. S. Levy and O. Nagai, Phys. Stat. Solidi (b) **93**, 351 (1979).
- <sup>5</sup> H. T. Diep, Phys. Stat. Solidi (b) , **103**, 809 (1981).
- <sup>6</sup> H. T. Diep, Phys. Rev. B **43**, 8509 (1991).
- <sup>7</sup> M.-C. Chung et al, Eur. Phys. J. B **18** 655 (2000).
- <sup>8</sup> J. Shen and al. Phys. Rev. **B** 56, 11134 (1997).
- <sup>9</sup> F. Rousseau and al. J. Vac. Sci Technol. B **13**, 2787 (1995).
- <sup>10</sup> L. Kong, L. Zhuang and S. Chu. IEEE Trans Magn **33**, 3019 (1997).
- <sup>11</sup> V. Grolier, J. Ferrr, A. Maziewski, E. Stefanowicz and D. Renard. J. Appl. Phys. **73**, 5939 (1993).
- <sup>12</sup> J. P. Jamet and al. Phys. Rev. **B** 57, 14320 (1998).
- <sup>13</sup> P. Meyer and al. Phys. Rev. Lett. **81**, 5656 (1998).
- <sup>14</sup> R. A. Tahir-Kheli and D. Ter Haar, Phys. Rev. **127**, 88 (1962).
- <sup>15</sup> C. Santamaria and H. T. Diep, J. Magn. Magn. Mater. **212**, 23 (2000).
- <sup>16</sup> C. Santamaria and H. T. Diep, J. Appl. Phys. , **91**, 6872 (2002).
- <sup>17</sup> N. N. Bogolyubov and S. V. Tyablikov, Doklady Akad. Nauk S.S.S.R. **126**, 53 (1959) [translation: Soviet Phys.-Doklady **4** 604 (1959)].
- <sup>18</sup> see for example R. Quartu and H.T. Diep, Phys. Rev. B **55**, 2975 (1997).
- <sup>19</sup> P. Fröbrich, P. J. Jensen and P. J. Kuntz, Eur. Phys. J B **13**, 477 (2000) and references therein.
- <sup>20</sup> D. N. Zubarev, Usp. Fiz. Nauk **187**, 71 (1960)[translation: Soviet Phys.-Uspekhi **3** 320 (1960)].
- <sup>21</sup> C. Santamaria, R. Quartu and H. T. Diep, J. Appl. Physics **84**, 1953 (1998).
- <sup>22</sup> H. Boubcheur, P. Massimino and H. T. Diep, J. Mag. Mag. Mater. **223**, 163 (2001) and references cited therein.
- <sup>23</sup> A. Zangwill, *Physics at Surfaces*, Cambridge University Press (1988).
- <sup>24</sup> *Ultrathin Magnetic Structures*, vol. I and II, J.A.C. Bland and B. Heinrich (editors), Springer-Verlag (1994).